RELATIONSHIP BETWEEN FOREST STAND PARAMETERS AND MULTI-BAND SAR BACKSCATTERING

Jung-il Shin*, Jong-suk Yoon, and Kyu-sung Lee

Department of Geoinformatic Engineering, Inha University
Jungil79@inhaian.net, ksung@inha.ac.kr

ABSTRACT ... Newly developing SAR (Synthetic Aperture Radar) sensors commonly include high resolution X-band those data are expected to contribute various applications. Recent few studies are presenting potential of X-band SAR data in forest related application. This study tried to investigate the relationship between forest stand parameters and multi-band SAR normalized backscattering. Multi-band SAR data was radiometric corrected to compare signal from different forest stand condition. Then correlation coefficients were estimated between attribute of forest stand map and normalized backscattering coefficients. Although overall correlation coefficients are not high, only X-band shows strong relationship with DBH class than other bands. The signal of C- and L-band is composed of a large number of discrete tree components such as leaves, stems, even background soil. In forest, strength of radar backscattering is affected by complex parameters. Further study might be considered more various forest stand parameters such as canopy density, stand height, volume, and biomass.

KEY WORDS: Synthetic Aperture Radar, Multi-band, Forestry, Signal characteristics

1. INTRODUCTION

Several new space-borne Synthetic Aperture Radar (SAR) sensors are recently developing those are commonly including high resolution X-band. Recently a few studies are presenting potential of X-band SAR data in various applications such as agriculture, marine science, glacier monitoring, even forestry (Baghdadi et al., 2008; Gade et al., 2008, Tedesco and Miller, 2007; Guglielmetti et al, 2007). Application of SAR data in forestry have been focused on the estimation of forest stand parameters such as canopy height, stand density, volume, and biomass (Neeff et al, 2005; Walker et al., 2007; Ranson et al., 1997). In conventional forest related applications, C-, L-, P-band SAR data were primarily used due to the penetration capability in tree canopy (Henderson and Lewis, 1998). However, SAR signal of each band may have different information because of different volume scattering location. Especially, X-band SAR signal is backscattered on top of the tree canopy (Jensen, 2000).

Backscattering coefficient is the ratio the power of the pulse transmitted and received (CREASO ©, 2007). Backscattering coefficient is classified by data processing level (Weber and Bodechtel, 1998). Firstly, the beta nought (β°) is the radar brightness coefficient in slant range. Secondly, the sigma nought (σ°) is the reflected strength of radar signals in horizontal plane which is significantly affected by incidence angle, wavelength and polarization. Lastly, the gamma (γ) is the normalized backscattering coefficient by the cosine of the incidence angle. Backscattering coefficient is needed to calibrate for comparison from different sensors, modes and incidence angle (CREASO ©, 2007; Lee, 1997).

Until now, radiometric correction methods are developing for mountainous area and also signal characteristics of SAR data are needed to study in forestry. In our previous study, we presented potential of multi-band SAR data for classifying forest cover type. As the second stage, this study aimed to investigate the relationship between forest stand parameters and multi-band SAR normalized backscattering. Multi-band SAR data was radiometric corrected to compare signal from different forest stand condition, Then correlation coefficients were estimated between attribute of forest stand and normalized backscattering coefficients.

2. STUDY AREA AND DATA

The study area is a mountainous national forest area near Seoul Metropolitan area, S. Korea. Since the study area has been well conserved by the Korea Forest Research Institute (KFRI), it has sufficient and accurate forest information database to verify samples from SAR data. Dominant tree species are oak (*Quercus*), larch (*Larix leptolepis*), and Korean pine (*Pinus koraiensis*) in 6x10km^{2}area.

Synthetic Aperture Radar data, SIR-C/X-SAR, was obtained simultaneously on 3rd October 1994. SIR-C data (C- and L-band) were obtained with dual-polarized (HH, HV) mode and X-SAR data were obtained with VV polarization. All five datasets (XVV, CHH, CHV, LHH and LHV) were almost identical value of incidence angle and look directions. Table 1 shows specification of three data sets over the study area.

Table 1. Specification of SIR-C/X-SAR data.

Sensor	SIR-C	X-SAR
Frequency(GHz)	5.304(C), 1.254(L)	9.602(X)
Polarization	HH, HV	VV
Date/Time(GMT)	Oct. 3, 1994 / 04:54:15.473	Oct. 3, 1994 / 04:54:18.240
Line/pixel spacing(m)	12.5 / 12.5	12.5 / 12.5
Orbital direction	Descending	Descending
Incidence angle at image center(deg.)	40.3460000	38.9921778

3. METHODS

3.1 Pre-processing of SIR-C/X-SAR data

As an initial process, SIR-C/X-SAR data were precisely geometric corrected for radiometric calibration. Because, side-looking radar image shows extreme terrain effect such as foreshortening and layover. RFM (Rational Function Model) was used for geometric correction with 70 GCPs and RMSE was 2.7pixels (33.75m). RFM is generic sensor model with high order polynomial equation which can be used to universal sensor even though some disadvantages such as low accuracy, instability, uncertainty and complexity (Dowmann and Dolloff, 2000). The simulated SAR image was used to collect GCPs which was generated with DEM, sensor altitude, heading direction and incidence angle information.

The SIR-C/X-SAR data were radiometric calibrated as suggested by the data distributor (DLR and ASI, 1995) to convert pixel's DN value to backscattering coefficients σ^o (1).

$$I = K_S \times \sin(\theta_i) \times \frac{\sigma^o}{\sin(\theta_i - \alpha)} + < N_{raw} > \times K_{N,0} \times K_N(i) \quad (1)$$

Where, $I = DN^2$, K_s = calibration constant, θ_i = incidence angle, σ^0 = backscattering coefficient, α = local terrain slope, $<N_{raw}>$ = average raw data noise power, $K_{N,0}$ = processor noise gain, $K_N(i)$ = cross-track radiometric correction vector(function of range). Precise geometric correction is essential pre-processing to calculate the local incidence angle $(\theta_i - \alpha)$.

Then, SIR-C/X-SAR image was terrain corrected by simple cosine correction method to get normalized backscattering coefficients (gamma). Terrain correction also important pre-processing to analyze surface characteristics due to radiometric distortion from terrain affects in SAR signal (Lee, 1997). Table 2 shows correlation coefficients between local incidence angle and mean backscattering coefficients from 23 samples of homogeneous forest stands that present the terrain effect on backscattering coefficients by processing level. Table 2 shows terrain effect on each band and X-band is less terrain effect than other bands. Figure 1 shows respectively uncorrected raw image, simulated SAR image, backscattering coefficients (σ^o) image after geometric correction and normalized backscattering coefficients (gamma) image by terrain correction of SIR-C/X-SAR CHH band. The uncorrected raw image (fig. 1a) and sigma nought (fig. 1c) show extreme terrain effect, but normalized backscattering coefficients image (fig. 1d) shows reduced terrain effect. Lastly, 3×3 size enhanced frost filter was used to reduce speckle noise.

Table 2. Correlation coefficients between local incidence angle and backscattering coefficients by processing level.

Band	Beta nought	Sigma nought	Gamma
XVV	-0.751	-0.817	-0.198
CHH	-0.924	-0.940	-0.519
CHV	-0.872	-0.907	-0.126
LHH	-0.864	-0.919	-0.510
LHV	-0.814	-0.889	-0.110

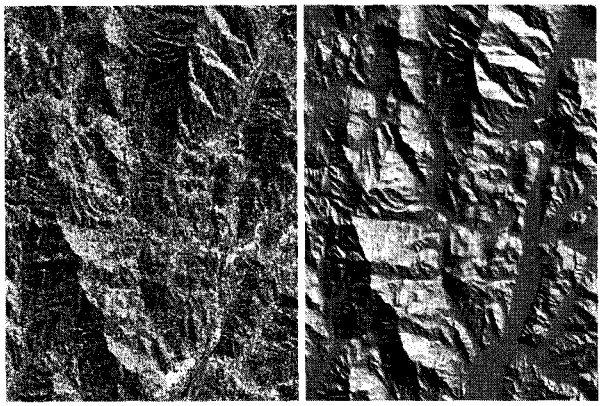

(a) uncorrected raw (b) simulated SAR

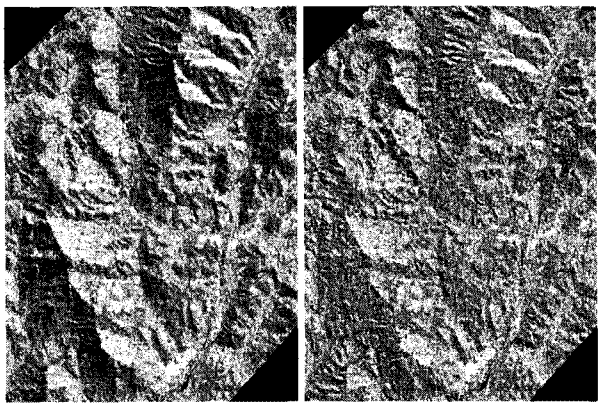

(c) geometric corrected (d) terrain corrected

Figure 1. SIR-C/X-SAR CHH band ; raw image (a), simulated SAR image with orbit altitude, heading direction and incidence angle (b), backscattering coefficients (σ^o) image after geometric correction by RFM (c), terrain corrected backscattering coefficients (gamma) image by simple sine correction (d).

3.2 Ground Sample Collection and Analysis Method

To investigate the characteristics of backscattering coefficients among X-, C-, L-bands in temperate forest, we collected totally 150 ground samples at center of the homogenous forest stands. The forest stand map was used

as reference that was generated by field measurement of KFRI in middle of 1990's. It has some rough forest stand attributes those are species, DBH (diameter at breast height) class, and age class. The attribute of forest stand map is related with forest stand parameters such as height, biomass. This initial study used attribute of forest stand map instead of forest stand parameter. Table 3 shows number of sample by attribute of forest stand. The ground samples were collected under consideration of area ratio.

The mean normalized backscattering coefficients were calculated with around 9 pixel values in terrain corrected image. Then, correlation coefficients (r) were computed between mean normalized backscattering coefficients and each parameter in each forest stand respectively band by band.

Table 3. Number of ground samples by attributes of forest stand map. ( ) is the symbol of species in forest stand map.

DBH class	Age class	Species		
		Oak (Q)	Larch (PL)	Korean pine (PK)
1	II	-	4	7
	III	4	10	11
	IV	8	1	5
	V	5	1	-
	VI	-	1	-
	VII	-	1	-
2	II	-	-	1
	III	-	1	4
	IV	-	2	4
	V	7	6	7
	VI	-	7	8
	VII	10	3	7
3	V	-	-	3
	VI	-	2	1
	VII	2	3	2
	VIII	-	4	8
Total (150)		36	46	68

4. RESULTS AND DISCUSSION

Correlation coefficients were estimated between mean normalized backscattering coefficients and age class or DBH class for each band. As the result of the analysis about relationship using correlation coefficients, only XVV band showed strong relationship between mean normalized backscattering coefficients and age class or DBH class in each band. Table 4 and 5 shows correlation coefficients between normalized backscattering coefficients with age class and DBH class respectively in species which present strong relationship with X-band. Otherwise, other bands (C-, L-band) didn't show any relationship with age class or DBH class. Figure 2 is scatter plots between age class and normalized backscattering coefficients (Gamma) in each band for Korean pine. XVV band (fig 2a) shows higher backscattering by increasing age class. But other bands (fig. 2 b and c) are shown relatively weak pattern than XVV band.

Table 4. Correlation coefficient (r) between age class and normalized backscattering coefficients.

Species	XVV	CHH	CHV	LHH	LHV
Q	0.864	0.439	0.539	0.301	0.265
PL	0.936	0.457	0.444	0.102	0.430
PK	0.945	0.331	0.124	0.254	0.312

* Q : *Quercus,* PL : *Larix leptolepis*, PK : *Pinus koraiensis.*

Table 5. Correlation coefficient (r) between DBH class and normalized backscattering coefficients.

Species	XVV	CHH	CHV	LHH	LHV
Q	0.667	0.428	0.447	0.246	0.151
PL	0.726	0.307	0.337	-0.026	0.297
PK	0.737	0.156	0.119	0.137	0.241

* Q : *Quercus,* PL : *Larix leptolepis*, PK : *Pinus koraiensis.*

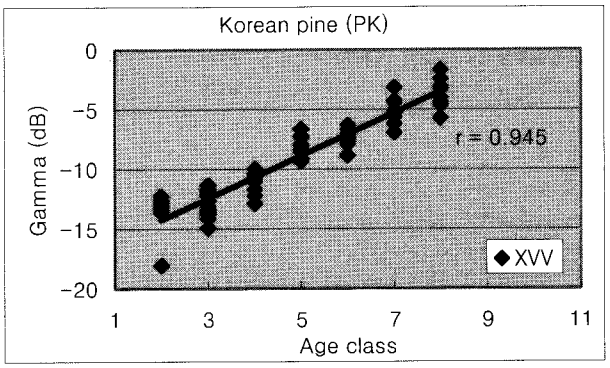

(a) XVV

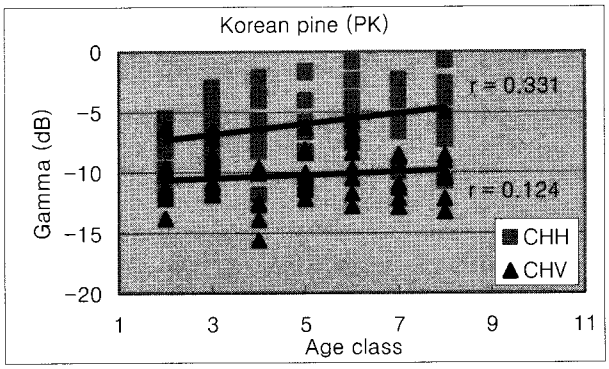

(b) CHH and CHV

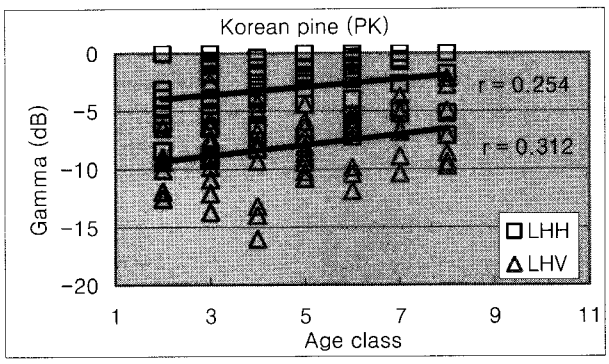

(c) LHH and LHV

Figure 2. Scatter plots between age class and normalized backscattering coefficients for Larch forest stand.

High correlation coefficients of X-band means that the signal of X-band is more sensitive to attribute of forest stand map. Although attribute of forest stand map is not continuous value and those can't explain directly forest stand parameters, some forest stand parameters could be estimated using empirical model locally with DBH and age. Stand height is expressed as polynomial of DBH and age. Also, volume could be expressed as tree height and DBH (KFRI, 1998). Some forest stand parameters such as canopy density and volume are related with amount of leaves which affect to penetration capability of XVV band due to short wavelength of X-band. On the other hands, the signal of other bands is composed of a large number of discrete tree components (leaves, stems, even background soil) by long wavelength. Because, in forest, strength of radar backscattering is affected by complex parameters such as wavelength, canopy density, size of leaves, moisture contents, polarization, alignment, and incidence angle (Lillesand et al., 2004).

5. CONCLUSION

In this study, the signal relationship was investigated between forest stand parameters and normalized backscattering of multi-band SAR. To compare signal from different forest stand condition, multi-band SAR data was radiometric corrected to terrain effect. Then correlation coefficients were estimated between attribute of forest stand map and normalized backscattering coefficients. The correlation coefficients of X-band only showed strong relationship with attribute of forest stand map. On the other hand, overall correlation coefficients of C- and L-band were not high. It means high sensitivity of X-band with DBH class and age class than other bands due to weak penetration capability of X-band. The signal of other bands is composed of a large number of discrete tree components such as leaves, stems, even background soil. In forest, strength of radar backscattering is affected by complex parameters as long as wavelength. Some forest stand parameters could be estimated using empirical models locally with field measured DBH and age. However classified DBH and age of forest stand map is not enough to explain directly signal characteristics of multi-band SAR data. Further study could be considered more various forest stand parameters such as canopy density, stand height, volume, and biomass. This study will be extended to the application of X-band SAR in forestry along with the expected launch of KOMPSAT-5 satellite.

6. REFERENCES

Baaghdadi, N., Zribi, M., Loumagne, C., Ansart, P., and Anguela, T., 2008. Analysis of TerraSAR-X data and their sensitivity to soil surface parameters over bare agricultural fields. *Remote Senisng of Environment*, In press.

Gade, M., Alpers, W., Melsheimer, C., and Tanck, G., 2008. Classification of sediments on exposed tidal flats in the German Bight using multi-frequency radar data. *Remote Senisng of Environment*, 112(4), pp. 1603-1613.

Tedesco, M. and Miller, J., 2007. Observations and statistical analysis of combined active–passive microwave space-borne data and snow depth at large spatial scales. *Remote Senisng of Environment*, 111(2), pp. 382-397.

Guglielmetti, M., Schwank, M., Mätzler, C., Oberdörster, C., Vanderborght, J., and Flühler, H., 2007. Measured microwave radiative transfer properties of a deciduous forest canopy. *Remote Senisng of Environment*, 109(4), pp. 523-532.

Neeff, T., Gracia, P., Dutra, L., and Freitas, C., 2005. Carbon budget estimation in central Amazonia : Successional forest modeling from remote sensing data. *Remote Sensing of Environment*, 94(4), pp. 508-522.

Walker, W., Kellndorfer, J., and Pierce, L., 2007. Quality assessment of SRTM C- and X-band interferometric data : Implications for the retrieval of vegetation canopy height. *Remote Sensing of Environment*, 106(4), pp. 428-448.

Ranson, K., Sun, G., Weishampel, J., and Knox, R., 1997. Forest Biomass from combined ecosystem and radar backscatter modelling. *Remote Sensing of Environment*, 59(1), pp. 118-133.

Henderson, F. and Lewis, A., 1998. Principal and Application of Imaging Radars – Manual of Remote Sensing. Volume 1, ASPRS, pp. 480-481.

Jensen, J., 2000. Remote sensing of the environment – an earth resource perspective, Prentice Hall, pp. 285-316.

CREASO ©, 2007, The SAR – Guidebook : Examples based on SARscape®, http://www.creaso.com/english/12_swvis/13_envi/SARscape/SAR-Guidebook.pdf

Wever, T., and Bodechtel, J., 1998. Different processing levels of SIR-C/X-SAR radar data for the correction of relief induced distortions in mountainous areas. *International Journal of Remote Sensing*, 19(2), pp. 349-357.

Lee, K., 1997, Topographic normalization of satellite Synthetic Aperture Radar (SAR) Imagery. *Journal of the Korean Society of Remote Sensing*, 13(1), pp. 57-73.

Dowman, I., and Dolloff, J., 2000. An evaluation of rational functions for photogrammetric restitution. *International Archives of Photogrammetry and Remote Sensing*, XXXIII(B3), pp. 254-266.

DLR and ASI, 1995. X-SAR CEOS format. DLR, pp. 1-33.

Lillesand, T., Kiefer, R., and Chipman, J., 2004. Remote sensing and image interpretation. John Wiley & Sons, New York, pp. 676-682.

Korea Forest Research Institute, 1998. Forest inventory report. Korea Forest Research Institute, pp. 4-15. http://book.kfri.go.kr/forest/resources/html/files/report14.pdf